Published in final edited form as:
Mol Cancer Ther. 2013 March ; 12(3): 255–263. doi:10.1158/1535-7163.MCT-12-0777.

A Second Generation 2-Methoxyestradiol Prodrug Is Effective Against Barrett's Adenocarcinoma in a Mouse Xenograft Model

Suman Kambhampati[1,2,#,*], **Roger A. Rajewski**[4,#], **Mehmet Tanol**[4,#], **Inamul Haque**[1,2,#], **Amlan Das**[1,2], **Snigdha Banerjee**[1,2], **Saheli Jha**[1,2,€], **Douglas Burns**[1], **Emma Borrego-Diaz Reyes**[1,2], **Peter J. Van Veldhuizen**[1,2], and **Sushanta K. Banerjee**[1,2,3,*]

[1]Cancer Research Unit, VA Medical Center, Kansas City, Missouri, USA

[2]Division of Hematology and Oncology, Department of Internal Medicine, University of Kansas Medical Center, Kansas City, Kansas, USA

[3]Department of Anatomy and Cell Biology, University of Kansas Medical Center, Kansas City, Kansas, USA

[4]Department of Pharmaceutical Chemistry, The University of Kansas, Lawrence, Kansas, USA

Abstract

2-Methoxyestradiol (2-ME2) is an endogenous metabolite of estradiol. In preclinical models, 2-ME2 is effective against different types of tumors. Unfortunately, only low systemic concentrations of 2-ME2 can be achieved following oral administration, even after very high doses are administered to patients. In an effort to solve this problem we have now synthesized and tested a new prodrug of 2-ME2 that is water soluble due to a bio-reversible hydrophilic group added at the 3-position and more effectively resists metabolic inactivation due to an ester moiety added to mask the 17-position alcohol. We are reporting here for the first time that this double prodrug of 2-ME2 is effective as an antiproliferative and anti-cancer agent for both *in vitro* and *in vivo* studies against Barrett's esophageal adenocarcinoma (BEAC), and provided greater potency than 2-ME2 in inhibiting the growth of BEAC xenografts. Finally, studies indicate that, like 2-ME2, the 2-ME2-PD1 exhibits anticancer effect through possible disruption of microtubule-network.

Keywords

2-Methoxyestradiol; Esophageal cancer; Chemotherapy; Prodrug

[*]To whom correspondence should be addressed: Cancer Research Unit, Research Division 151, VA Medical Center, 4801 Linwood Boulevard, Kansas City, Missouri 64128, USA. Phone: (816) 861-4700 ext. 57057/57075, FAX: (816) 922-3320, skambhampati@kumc.edu/sbanerjee2@kumc.edu/publication@vamccancerresearchunit.org.
[#]These authors contributed equally to the work described in this manuscript.
[€]**Present Address:** National Institute of Diabetes and Digestive and Kidney Diseases, Gene Expression and Regulation Section, NIH, Bethesda, USA

Disclosure of Potential Conflict of Interest: No potential conflict of interest were disclosed

Introduction

2-ME2 is an endogenous metabolite of 17β-estradiol (E2), which is generated from a two-step activation process involving sequential hydroxylation at the 2C position of 17β-estradiol by cytochrome P450 enzymes followed by methylation at the same position by catechol-*O*-methyl transferase (COMT) (1, 2). Our laboratory has studied the anticancer activities of 2-ME2 for many years (3-6). In addition, multiple *in vitro* and *in vivo* studies have documented that 2-ME2 is effective against many different types of tumors by virtue of its potent antiproliferative, antiangiogenesis and proapoptotic activities (7-9).

Despite the great promise and broad anticancer properties demonstrated for exogenous 2-ME2, clinical application is limited because the *in vivo* effect of 2-ME2 is inconsistent and weak due to poor bioavailability of the 2-ME2. The published literature identifies very high patient-to-patient variability in systemic exposure following oral administration. In all cases there is low serum bioavailability (approximately 1 - 2%) and a limited temporal window with measurable serum levels (1, 10-12). Thus, high oral doses of 2-ME2 that present dosing challenges would be necessary to maintain therapeutic level of the drug in the plasma for effective lengths of time.

The major barriers to oral delivery of 2-ME2 to systemic circulation include, but are not limited to, formulation, solubility, permeability, transporter effects, and first-pass metabolism (1). Prodrug approaches have been employed with varying degrees of success to overcome all these barriers (13-15). Thus, designing a prodrug of 2-ME2 would be one promising approach to solving the problem of oral delivery. A prodrug is a chemically modified drug designed to be endogenously converted to the active drug. Unfortunately, prior studies devoted to the design and testing of 2-ME2 prodrugs have not produced a successful chemotherapeutic agent (1).

Building on the successes and limitations noted for the first generation of 2-ME2 analogues, we devised a strategy to create improved 2-ME2 prodrugs that exhibit more predictable pharmacokinetics. In summary, we describe the synthesis of a novel prodrug that, by virtue of its initial assessments, promises to be an effective oral anticancer agent against esophageal cancer.

Materials and Methods

Cell line

OE33 cells, was purchased from American Type Culture Collection (ATCC; Manassas, VA). OE33 cells used in this study were from 5th through 10th passages and were routinely maintained in Dulbecco's modified Eagle's medium ((DMEM), Sigma, St Louis, MO) supplemented with 10% fetal bovine serum (Hyclone, Logan, UT) and antibiotics (Sigma), penicillin (100 U/mL), and streptomycin (100μg/ml). The cell line authentication and the status of mycoplasm were carefully determined before and after performing the experiments needed for these studies. In these studies, we used only one cell line as widely used BEAC cell lines (i.e., BIC-1, SEG-1 and TE-7) are in serious identity crisis (16, 17). FLO-1 cell

line, which has been utilized for various studies as evidenced by citations in PubMED, and has been authenticated with the parental tumor, is unavailable now in ATCC.

Reagents

The 2-ME2 was purchased from Sigma (St. Louis, MO), and 20 μM stock solutions of 2-ME2 were prepared in absolute ethyl alcohol and stored at -20°C. All other chemical were obtained either from Sigma (St. Louis, MO) or Fisher Scientific (Fisher Scientific Company, Fair Lawn, NJ). All newly synthesized compounds were characterized by using analytical tools.

Animals

Fasted Sprague Dawley rats (male, 250-300 mg) were purchased from Charles River Laboratories. Six- to 8-wks-old athymic male athymic nude mice (BALB/c-nu/nu) were obtained from Charles River Laboratories. All animals were maintained in a sterile environment and daily 12-h light/12-h dark cycle. All the animals were maintained according to standard guidelines of American Association for the Accreditation of Laboratory Animal Care with the approval of the Institutional Animal Care and Use Committee of the Kansas City VA Medical Center, Kansas City, MO and the University of Kansas, Lawrence, KS.

Rationale for the Design of the 2-ME2 Prodrug

2-ME2 is a poorly soluble compound with a predicted aqueous solubility of 4.8 micrograms/mL (calculated using the Advanced Chemistry Development Software V8.14 for Solaris). 2-ME2 possesses poor aqueous solubility over the complete pH profile of the gastrointestinal tract. Since bioavailability has been increased through recent developments in nanocrystal formulation (10-K SEC Filing, filed by Entremed Inc. on 3/6/2008), there is evidence suggesting that a more soluble form of 2-ME2 would help increase its absolute bioavailability.(1, 11). Thus, to overcome the unpredictable pharmacokinetics of the parent 2-ME2 compound, the synthetic efforts have been focused on (i) increasing the aqueous solubility/dissolution rate through the addition of a bioreversible hydrophilic group at the 3-position and (ii) altering drug metabolism by masking the 17-position through covalent addition of an ester moiety (Fig. 1).

Synthesis of the 2-ME2 Prodrug (2-ME2-PD1)

The synthesis of the main compound, 2-ME2-PD1 - disodium (((8R,9S,13S,14S,17S)-17-acetoxy-2-methoxy-13-methyl-7,8,9,11,12,13,14,15,16,17-decahydro-6H-cyclopenta[a]phenanthren-3-yl)oxy)methyl phosphate ($C_{22}H_{29}Na_2O_8P$) is as follows (Fig. 1).

Step 1: 300 mg (8R,9S,13S,14S,17S)-2-methoxy-13-methyl-7,8,9,11,12,13,14,15,16,17-decahydro-6H-cyclopenta[a]phenanthren-17-ol (2-methoxy estradiol; 0.1 mmol) and 0.140 mL chloromethyl methyl sulfide (1.67 mmol) were dissolved in 20-mL of dry dimethylformamide. 150 mg of 60% sodium hydride was added. The mixture was stirred at room temperature for one hour. Next the solvent was removed *in vacuo* and the resulting solids dissolved in ethyl acetate. The organic layer was washed with water then filtered

through silica gel. The ethyl acetate was removed *in vacuo*. The solids were dissolved in a 1:2 v/v mixture of ethyl acetate and hexanes and the major product isolated with elution on a silica gel column with the same solvents (Rf =0.45) to provide 313 mg (8R,9S,13S,14S, 17S)-2-methoxy-13-methyl-3-((methylthio)methoxy)-7,8,9,11,12,13,14,15,16,17-decahydro-6H-cyclopenta[a]phenanthren-17-ol (Precursor 1; 86% yield).

Step 2: 208 mg of MTM 2-ME2 (0.57 mmol) and 126 mg acetic anhydride (1.23 mmol, 3 eqv.) were dissolved in 10-mL dry pyridine at 0°C. The reaction was stirred overnight and allowed to come to room temperature. The solvent was removed *in vacuo* and the resulting solid was dissolved in a 1:2 v/v mixture of ethyl acetate and hexanes. The major product was isolated with elution on a silica gel column with the same solvents (Rf = 0.81) to provide 157 mg (8R,9S,13S,14S,17S)-2-methoxy-13-methyl-3-((methylthio)methoxy)-7,8,9,11,12,13,14,15,16,17-decahydro-6H-cyclopenta[a]phenanthren-17-yl acetate (Precursor 2; 68% yield).

Step 3: 157 mg of OAc MTM 2-ME2 (0.39 mmol), 325 mg dibenzyl hydrogen phosphate (1.16 mmol, 3 eqv.), and 320 mg *N*-iodosuccinimide (1.42 mmol, 3.6 eqv.) were dissolved in 5-mL of dry tetrahydrofuran at room temperature. After one hour, the reaction was stirred and the solvent was removed *in vacuo*. The resulting solid was dissolved in a 1:2 v/v mixture of ethyl acetate and hexanes and the major product isolated with elution on a silica gel column with gradient elution (1:2 v/v ethyl acetate:hexanes to 1:1 v/v ethyl acetate:hexanes; Rf = 0.62) to provide 120 mg (8R,9S,13S,14S,17S)-3-(((bis(benzyloxy)phosphoryl)oxy)methoxy)-2-methoxy-13-methyl-7,8,9,11,12,13,14,15,16,17-decahydro-6H-cyclopenta[a]phenanthren-17-yl acetate (Precursor 3; 49% yield).

Step 4: 50 mg of Dibenzyl phosphate OAc MTM 2-ME2 (0.079 mmol) was dissolved in a mixture of 2 mL water and 25 mL tetrohydrofuran at room temperature. 11 mg disodium carbonate monohydrate and 50 mg 10% palladium on carbon were added and the reaction was stirred two hours under hydrogen at atmospheric pressure. The mixture was then filtered through a 0.45 micron Nylon filter and lyophilized to provide 39 mg of the title compound (2-ME2-PD1; 100% yield). Identity was confirmed by mass spectroscopy using a Shimadzu 2010 single quadrupole spectrometer in negative ion mode (free acid theoretical mass: 454.45 amu, found M-1 at 452.95 amu).

Pharmacokinetic Analysis of 2-ME2-PD1 and 2-ME2

2-ME2-PD1 and 2-ME2 were dissolved independently in 0.2 M hydroxypropyl-β-cyclodextrin (Sigma-Aldrich) or 0.1 M Captisol® (Ligand Pharmaceuticals, Inc) at concentrations between 10 mg/mL and 21 mg/mL. The solutions were sterile filtered through 0.2 micron filters prior to use. A cannulated rat model was used to study the intravenous (iv) and oral absorption of 2-ME2 and 2-ME2-PD1. Sprague Dawley rats were implanted with carotid artery, and jugular and/or femoral vein catheters. These studies were automated with the animals connected to the Culex Automated Pharmacology System allowing for direct comparison of pharmacokinetic behavior between the orally and intravenously administered compounds in the same animal. Following surgery, the animals were connected to the Culex and allowed to recover and acclimate.

Oral doses were given via gavage to the animal under light anesthesia. Blood was sampled at times ranging from 5 to 1440 minutes into heparinized vials containing a cocktail of phosphatases and esterase inhibitors stored on the chilled fraction collector, and remained there until sampling was complete. Blood samples were processed to plasma via centrifugation and stored at -80 °C until analysis for 2-ME2-PD1, 2-ME2 and associated metabolite concentrations by liquid chromatography-mass spectrometry (LC-MS/MS). Bioanalytical methods for the 2-ME2-PD1 and 2-ME2 analysis were modified from those of Lakhani et al (18). Quantitation was made relative to deuterated internal standards. Pharmacokinetic analysis of the resulting plasma concentration time data was performed using PK Solutions software (Summit PK).

In vitro cell proliferation assay

The antiproliferative effect of 2-ME2 and 2-ME2-PD1 on OE33 cells was evaluated using crystal violet cell proliferation assay according to previous method (19). Eight duplicate wells were used for each determination. Inhibition of cell proliferation was calculated as a percentage using following equation-

$$\%\text{of inhibition}=(1-\text{OD of the treated sample}/\text{OD of the vehicle treated sample})\times 100.$$

Induction and treatment of tumor xenograft and sample collection

OE33-tumor xenografts were generated essentially as previously described (20, 21). Briefly, semiconfluent OE33 cells (2.5×10^6) were re-suspended in Matrigel and were injected *sc* into the right hind leg of each mouse for the development of the tumor. The animals were distributed into three groups (5 mice/group). After detection of palpable tumor, mice were given daily equivalent doses of 2-ME2 or 2-ME2-PD1 (75 mg/kg/day) by orogastric feeding or vehicle (control). 2-ME2-PD1 was dissolved in saline water + peptamen (Nestle) and 2-ME2 was dissolved in DMSO + peptamen (milk) in an appropriate ratio. The control group was given an equal volume of peptamen. Tumor growth was monitored by measuring two perpendicular diameters twice weekly. Tumor volume was calculated according to the formula $V= a \times b^2/2$, where *a* is length and *b* is width, respectively. All mice were killed after 12 d of treatment. Tumors were isolated carefully and were immediately fixed in 4% neutral-buffered formalin, placed in fixative overnight, embedded in paraffin and sectioned at 5 μm intervals before immunofluorescence analysis.

Immunofluorescence

The immunofluorescence procedure was the same as previously described (21, 22). Briefly, for *in vitro* analysis, OE33 cells were fixed with acetone and permeabilized with 0.1% Triton X-100. For *in vivo* analysis, tumor xenograft paraffin-embedded tissue sections were deparaffinized and then rinsed in distilled water. Nonspecific binding sites were blocked by Super Block Blocking Buffers (Thermo) followed by incubation with rabbit monoclonal anti-α-Tubulin (Alexa Fluor® 555 Conjugate) and counter stained with DAPI. Images were captured by a Nikon Eclipse Ti-U fluorescence microscope.

Statistical Analysis

Analyses of data were achieved with GraphPad Prism version 4.00, GraphPad Software, San Diego California USA. All data are expressed as the mean ± SD. Statistically significant differences between groups were determined by using the paired Student's two-tailed *t*-test. A value of $P < 0.05$ was considered statistically significant.

Results

Pharmacokinetics of 2-ME2 prodrug (2-ME2-PD1) relative to 2-ME2

2-ME2-PD1 was synthesized in 28% overall yield, starting from 2-ME2 as precursor. Unlike 2-ME2, 2-ME2-PD1 readily dissolves in sterile water for easy use and rapid preparation of doses. Validation studies with the phosphatase and esterase inhibitors demonstrated the stability of 2-ME2-PD1 and its ester metabolite in whole blood following sampling. There were no observable effects in the animals following dosing of 2-ME2-PD1 and 2-ME2 in the pharmacokinetic studies. Non-parametric analysis of the resulting plasma concentration-time data was performed and the pharmacokinetic parameters were derived following the standard methods (23), (Fig. 2 and Tables S1 and Table 1). For oral doses of 2-ME2, no compound could be detected in plasma at any time point studied using Limit of Quantification (LOQ; < 2 ng/mL) demonstrating again the limited bioavailability of oral 2-ME2. Intravenous 2-ME2 dosing does produce measurable drug levels in plasma, but these levels are short-lived due to presumed rapid clearance (Table 1). Our data suggest that the strategy employed to develop 2-ME2-PD1 does deliver meaningful levels of 2-ME2 to the systemic circulation for extended periods of time following either oral or intravenous administration. The studies demonstrate that therapeutic levels of 2-ME2 are sustained for at least 240 minutes, and significant amounts are present for as long as 480 minutes for the higher doses (31.5 mg/kg of orally administered 2-ME2-PD1) (Fig. 2). This suggests, in these limited studies, that the oral bioavailability of 2-ME2-PD1 appears to be dose-dependent. No analyzed sample displayed detectable levels of 2-ME2 when plasma was analyzed at times greater than 480 minutes.

These experiments demonstrate that oral 2-ME2-PD1 administration results in a higher systemic exposure relative to 2-ME2. The absolute bioavailability of orally administered 2-ME2-PD1 relative to intravenous administration of 2-ME2 is in the 4-5% range. A plasma half-life of 262 minutes is obtained for intravenous 2-ME2-PD1 as opposed to 59 minutes for a comparable intravenous dose of 2-ME2. Orally, 2-ME2-PD1 produces far superior results compared to 2-ME2 and yields a 2-ME2 plasma half-life of 411 to 807 minutes, which is a marked improvement over what can be obtained with 2-ME2 itself. These data suggest that more detailed and extensive studies should be conducted to further establish our proof-of-concept for this new prodrug.

The effect of 2-ME2-PD1) on viability of OE33 cells relative to 2-ME2

Previously, we demonstrated that 2-ME2 dose-dependently inhibits the BEAC cell proliferation and the 50% inhibitory concentration (IC_{50}) was ∼ 5 μM of 2-ME2 (21). In this study, we sought to determine if 2-ME2-PD1 exhibits similar effect on the viability of OE33 cells. To do so, OE33 cells were treated with either 2-ME2-PD1 or 2-ME2 at various

concentrations for 48 hours followed by crystal violet dye colorimetric assay for the viability of OE33 cells. As shown in Fig. 3, a dose-dependent inhibition of OE33-proliferation was observed when the cells were exposed to 2-ME2 or 2-ME2-PD1 but 2-ME2 is much more potent than the pro-drug. The IC_{50} for 2-ME2 was found to be approximately 6 μM after 48 h of incubation while for the prodrug the IC_{50} was obtained at approximately 17 μM, indicating that the prodrug provides significantly less *in vitro* antiproliferative effect on OE33 cells as compared to the parent 2-ME2.

Alteration in Cellular Morphology of OE33 Cells by 2-ME2 and 2-ME2-PD1-treatment

Morphological alterations such as vacuolation and atrophy due to membrane blebbing, and cytoplasmic shrinkage are the common cytotoxic effects of an anticancer drug (24, 25). We therefore investigated whether 2-ME2 and 2-ME2-PD1 are able to alter the cellular morphology of OE33 cells. To test this, the phase contrast images of the treated and untreated cells were studied (Fig. 4A-D). Untreated OE33 cells showed that cells were closely arranged with uniform size, as well as good viability with retained shape, morphology and refractivity after 48 h of culture (Fig. 4A), while aberrations in the cellular morphology were observed in both 2-ME2 and 2-ME2-PD1 treated cells in a dose-dependent fashion. In the presence of 2.5 μM of -2-ME2-PD1 only mild to no alterations in the cellular morphology were observed (Fig. 4B), but when exposed to 5 μM of 2-ME2-PD1, the cells displayed atrophy (Fig. 4C). In contrast, the effect of each concentration of 2-ME2 (i.e., 2.5 μM or 5 μM), on cellular morphology was much more drastic as compared to 2-ME2-PD1 treated (Fig. 4D).

Disruption of the Microtubule Network in OE33 Cells by 2-ME2 and 2-ME2-PD1 treatment

Since anti-mitotic and anti-proliferative action of 2-ME2 is mediated via microtubule disruption (26), we sought to determine whether the cellular microtubule network also acts as a target for the 2-ME2-PD1 actions. To do so, immunofluorescence against α-Tubulin in 2-ME2-treated, 2-ME2-PD1-treated or untreated OE33 cells was performed to determine whether the prodrug is mimicking the function of 2-ME2 under similar *in vitro* conditions. In untreated OE33 cells organized microtubules were observed with characteristic fibrous network (Fig. 4E). Microtubule disruption was not very prominent in OE33 cells when treated with 2.5 μM 2-ME2-PD1 for 48h (Fig. 4F), but in the presence of 5 μM 2-ME2-PD1 (Fig. 4G) the organized microtubule structure was significantly disrupted with the gradual disappearance of the fibrous network like microtubule structure as observed in untreated cells (Fig. 4E). Consistent with the previous findings (26), we observed that in the presence of 5 μM 2-ME2 cellular microtubules were totally disrupted in OE33 cells (Fig. 4F). Taken together, these results underscore that the anti-proliferative effects of 2-ME2-PD1 on OE33 cells mimics 2-ME2 actions in a dose-dependent fashion, and provide proof that 2-ME2-PD1, although less effective than 2-ME2, retains the anti-microtubule disruptive anti-cancer properties of its parent drug, 2-ME2.

The effect of 2-ME2-PD1 on OE33 xenograft tumors relative to 2-ME2

In the next set of experiments we compared the *in vivo* effects of 2-ME2-PD1 with 2-ME2 on OE33 xenograft tumors. As illustrated in Fig. 5, our data shows that 2-ME2-PD1 strongly

and consistently, in a time-dependent fashion, inhibited the growth of established OE33 xenografts tumors in nude mice after 12 days of treatment as compared to the control group as well as 2-ME2 treated group where the effect was inconsistent. The parental 2-ME2 effect is in agreement with our previous work (21). Tumor size increased much more rapidly in the control animals relative to prodrug-treated group. Thus, the studies indicate that the prodrug appeared to provide better antitumor activity than did the parent compound in these experiments.

Because our *in vitro* studies showed that both 2-ME2 and 2-ME2-PD1 alter cellular morphology and microtubules distribution in OE33 cells, we investigated whether prodrug similarly affects on cellular morphology and microtubule networking under *in vivo* microenvironment. To do so, the distribution of microtubules was characterized in 2-ME2-PD1-treated and untreated tumor-xenograft-sections by immunofluorescence analysis using anti-α-Tubulin antibody. Consistent with *in vitro* data (Fig. 4), studies show striking alteration in microtubule distribution in conjunction with cellular morphology suggestive of mesenchymal (spindle-shaped) to epithelial (cuboidal) transition (MET) in 2-ME2-PD1 treated OE33-tumor xenografts as compared to untreated samples (Fig. 6).

Discussion

The present study effectively formulated a novel prodrug of 2-ME2 (2-ME2-PD1) and tested its antiproliferative and antitumorigenic efficacy in BEAC tumor models. The studies show that unlike parent 2-ME2, the 2-ME2-PD1 is water soluble, and the bioavailability of orally administered 2-ME2-PD1 is significantly higher as compared to intravenous and/or oral administration of 2-ME2 (Fig. 2). Although the 2-ME2-PD1 does not inhibit the *in vitro* growth of BEAC cells as effectively as parent 2-ME2 does (Fig. 3), the antitumorigenic action of 2-ME2-PD1 on BEAC xenograft is highly and significantly effective than the parent molecule (Fig. 5). Moreover, the antitumorigenic effect 2-ME2-PD1 on BEAC cells, like 2-ME2, is predominantly mediated through altering the microtubule networks as well as morphological changes from mesenchymal to epithelial type (Fig. 4 and 6).

Esophageal cancer remains a leading cause of cancer mortality worldwide, and in the United States it is the seventh leading cause of cancer death (27). Thus, there is an urgent need to investigate effective and less-toxic chemotherapeutic options to effectively combat this dangerous cancer. In pursuit of this goal, we have studied the anti-tumor properties of 2-ME2 in our laboratory for many years. We and others have found this compound to be effective against many different types of cancer (3, 4, 21, 28-30). Unfortunately, due to the limited aqueous solubility and less bioavailability, very high oral doses of 2-ME2 are needed to maintain therapeutic plasma levels of drug for an effective length of time, which is a great hindrance to its use as an anticancer drug (1, 10, 31, 32). Thus, designing the proper prodrug to defeat first-pass metabolic inactivation seems to be the best approach in developing a practical therapeutic agent from 2-ME2.

To advance our earlier work focused on BEAC, we undertook the task of designing a better prodrug of 2-ME2 by following a two-prong strategy directed at increasing aqueous solubility through addition of a bio-reversible hydrophilic group at the 3-position and then

altering *in vivo* metabolism by masking the 17-position through the covalent addition of an ester moiety (Fig. 1). The 3-position promoiety is designed to be cleaved at the brush-border of the intestinal epithelium providing high local concentrations of the prodrug intermediate for intestinal absorption. On the first-pass through the intestinal epithelium and liver, the masked 17-position will undergo de-esterification. Our results show that oral administration of this double 2-ME2 prodrug, 2-ME2-PD1, provides an absolute bioavailability of 4-5% (Fig. 2), and this is a significant improvement over what is observed with oral 2-ME2 and the first generation prodrugs of 2-ME2 (1). The first generation prodrugs did not include a methylene spacer between the alcohol and the phosphate ester group. The addition of the spacer greatly increases the ability of phosphatases to cleave the phosphate ester enroute to the generation of 2-ME2.

It is noteworthy that 2-ME2-PD1 is easily dissolved in sterile water for injection, and this made the prodrug much easier to use for in vitro dosing than 2-ME2, which being non-aqueous is usually dissolved in DMSO. In the *in vitro* experiments, comparison between the effect of 2-ME2 and the 2-ME2-PD1 on the viability of OE33 cells showed that the IC_{50} values of the 2-ME2-PD1 were ∼3-fold higher than those of 2-ME2 (Fig. 3). Although the *in vitro* mechanisms of 2-ME2-PD1 are not yet fully known, these results suggest that the active compound, 2-ME2, is being generated at the cellular level. This is not unexpected as alkaline phosphatase is present in cellular membranes and esterases are prevalent intracellularly. However, at the cellular level we have not yet determined whether through enzyme-mediated hydrolysis the prodrug is being converted to 2-ME2, and if so, it would be helpful to know the actual efficiency at which this conversion occurs.

The results of our *in vivo* experiments indicate that 2-ME2-PD1 has potent antitumor activity against BEAC xenograft tumor in nude mice over 12 days. An oral dose of 75 mg/kg/d of 2-ME2-PD1 significantly inhibit the growth of OE33-induced tumors in nude mice with reduction in tumor volume of 60 ± 5% relative to the control group and 2-ME2 group as well (Fig. 5). This result is highly significant as the prodrug dose is equivalent to a 45.5 mg/kg/d dose of 2-ME2. More simply stated, the prodrug dosed at 60% the level of 2-ME2 produced significantly higher reduction in tumor volume relative to 2-ME2. Thus confirming that, as compared to tissue culture conditions, in the enzyme-rich environment of the OE33-tumor xenografted animals there is more efficient and preferential conversion of 2-ME2-PD1 into systemically bioavailable 2-ME2.

Under *in vitro* conditions, 2-ME2 is known to inhibit the polymerization of the purified tubulin (26, 33) and impair microtubule dynamics (34) to mediate its tumor-suppressive actions on cancer cells. Here we report that the anti-proliferative effects of 2-ME2-PD1 on OE33 cells mimic those of its parent derivative, 2-ME2, and we provide evidence that these effects are pharmacodynamically mediated by the 2-ME2-PD1 induced dose-dependent alteration of the microtubule network as well as cellular architecture of these cells (Fig. 4 and 6). Normally, the morphology of OE33 cells is spindle-shaped of mesenchymal type. However, following treatment with parental 2-ME2 or 2-ME2-PD1, the morphology drastically changes from mesenchymal to an epithelial architecture (MET) (Fig. 4 and 6). Future studies are warranted to study the signaling pathways that are involved in 2-ME2-PD1 mediated MET event.

In summary, 2-ME2-PD1 functions as an effective prodrug that greatly improves the oral bioavailability of 2-ME2 and thus provides a unique opportunity for more focused development of 2-ME2-PD1 as chemotherapy for BEAC.

Supplementary Material

Refer to Web version on PubMed Central for supplementary material.

Acknowledgments

The authors thank all the members of CRU for their help in generating this manuscript.

Financial support: This work is supported by a VA VISN 15 Grant to SK, Merit review grants from the Department of Veterans Affairs (to S. Kambhampati, S. Banerjee and S. K. Banerjee), and the Kansas Technology Enterprise Corporation through the Centers of Excellence Program (to RAR and MT). This work is also supported by grants from the National Center for Research Resources (5P30 RR030926-03) and the National Institute of General Medical Sciences (8P30 GM103495-03) from the National Institutes of Health, and the State of Kansas (to SK).

References

1. Verenich S, Gerk PM. Therapeutic promises of 2-methoxyestradiol and its drug disposition challenges. Mol Pharm. 2010; 7:2030–9. [PubMed: 20831190]
2. Wilhelmson AS, Bourghardt-Fagman J, Gogos JA, Fogelstrand P, Tivesten A. Catechol-O-methyltransferase is dispensable for vascular protection by estradiol in mouse models of atherosclerosis and neointima formation. Endocrinology. 2011; 152:4683–90. [PubMed: 22009725]
3. Zoubine MN, Weston AP, Johnson DC, Campbell DR, Banerjee SK. 2-methoxyestradiol-induced growth suppression and lethality in estrogen-responsive MCF-7 cells may be mediated by down regulation of p34cdc2 and cyclin B1 expression. Int J Oncol. 1999; 15:639–46. [PubMed: 10493943]
4. Banerjee SN, Sengupta K, Banerjee S, Saxena NK, Banerjee SK. 2-Methoxyestradiol exhibits a biphasic effect on VEGF-A in tumor cells and upregulation is mediated through ER-alpha: a possible signaling pathway associated with the impact of 2-ME2 on proliferative cells. Neoplasia. 2003; 5:417–26. [PubMed: 14670179]
5. Ray G, Dhar G, van Veldhuizen PJ, Banerjee S, Saxena NK, Sengupta K, et al. Modulation of cell-cycle regulatory signaling network by 2-methoxyestradiol in prostate cancer cells is mediated through multiple signal transduction pathways. Biochemistry. 2006; 45:3703–13. [PubMed: 16533053]
6. van Veldhuizen PJ, Ray G, Banerjee S, Dhar G, Kambhampati S, Dhar A, et al. 2-Methoxyestradiol modulates beta-catenin in prostate cancer cells: a possible mediator of 2-methoxyestradiol-induced inhibition of cell growth. Int J Cancer. 2008; 122:567–71. [PubMed: 17935127]
7. Klauber N, Parangi S, Flynn E, Hamel E, D'Amato RJ. Inhibition of angiogenesis and breast cancer in mice by the microtubule inhibitors 2-methoxyestradiol and taxol. Cancer Res. 1997; 57:81–6. [PubMed: 8988045]
8. Fotsis T, Zhang Y, Pepper MS, Adlercreutz H, Montesano R, Nawroth PP, et al. The endogenous oestrogen metabolite 2-methoxyoestradiol inhibits angiogenesis and suppresses tumour growth. Nature. 1994; 368:237–9. [PubMed: 7511798]
9. Mueck AO, Seeger H. 2-Methoxyestradiol--biology and mechanism of action. Steroids. 2010; 75:625–31. [PubMed: 20214913]
10. Sweeney C, Liu G, Yiannoutsos C, Kolesar J, Horvath D, Staab MJ, et al. A phase II multicenter, randomized, double-blind, safety trial assessing the pharmacokinetics, pharmacodynamics, and efficacy of oral 2-methoxyestradiol capsules in hormone-refractory prostate cancer. Clin Cancer Res. 2005; 11:6625–33. [PubMed: 16166441]

11. Tevaarwerk AJ, Holen KD, Alberti DB, Sidor C, Arnott J, Quon C, et al. Phase I trial of 2-methoxyestradiol NanoCrystal dispersion in advanced solid malignancies. Clin Cancer Res. 2009; 15:1460–5. [PubMed: 19228747]
12. Liu Q, Jin W, Zhu Y, Zhou J, Lu M, Zhang Q. Synthesis of 3′-methoxy-E-diethylstilbestrol and its analogs as tumor angiogenesis inhibitors. Steroids. 2012; 77:419–23. [PubMed: 22280958]
13. Rautio J, Kumpulainen H, Heimbach T, Oliyai R, Oh D, Jarvinen T, et al. Prodrugs: design and clinical applications. Nat Rev Drug Discov. 2008; 7:255–70. [PubMed: 18219308]
14. Baudy RB, Butera JA, bou-Gharbia MA, Chen H, Harrison B, Jain U, et al. Prodrugs of perzinfotel with improved oral bioavailability. J Med Chem. 2009; 52:771–8. [PubMed: 19146418]
15. Ninomiya M, Tanaka K, Tsuchida Y, Muto Y, Koketsu M, Watanabe K. Increased bioavailability of tricin-amino acid derivatives via a prodrug approach. J Med Chem. 2011; 54:1529–36. [PubMed: 21319803]
16. Alvarez H, Koorstra JB, Hong SM, Boonstra JJ, Dinjens WN, Foratiere AA, et al. Establishment and characterization of a bona fide Barrett esophagus-associated adenocarcinoma cell line. Cancer Biol Ther. 2008; 7:1753–5. [PubMed: 18787394]
17. Boonstra JJ, van MR, Beer DG, Lin L, Chaves P, Ribeiro C, et al. Verification and unmasking of widely used human esophageal adenocarcinoma cell lines. J Natl Cancer Inst. 2010; 102:271–4. [PubMed: 20075370]
18. Lakhani NJ, Lepper ER, Sparreboom A, Dahut WL, Venitz J, Figg WD. Determination of 2-methoxyestradiol in human plasma, using liquid chromatography/tandem mass spectrometry. Rapid Commun Mass Spectrom. 2005; 19:1176–82. [PubMed: 15818726]
19. Menendez JA, Vazquez-Martin A, Garcia-Villalba R, Carrasco-Pancorbo A, Oliveras-Ferraros C, Fernandez-Gutierrez A, et al. tabAnti-HER2 (erbB-2) oncogene effects of phenolic compounds directly isolated from commercial Extra-Virgin Olive Oil (EVOO). BMC Cancer. 2008; 8:377. [PubMed: 19094209]
20. Ray G, Banerjee S, Saxena NK, Campbell DR, Van VP, Banerjee SK. Stimulation of MCF-7 tumor progression in athymic nude mice by 17beta-estradiol induces WISP-2/CCN5 expression in xenografts: a novel signaling molecule in hormonal carcinogenesis. Oncol Rep. 2005; 13:445–8. [PubMed: 15706414]
21. Kambhampati S, Banerjee S, Dhar K, Mehta S, Haque I, Dhar G, et al. 2-methoxyestradiol inhibits Barrett's esophageal adenocarcinoma growth and differentiation through differential regulation of the beta-catenin-E-cadherin axis. Mol Cancer Ther. 2010; 9:523–34. [PubMed: 20197389]
22. Das A, Chakrabarty S, Choudhury D, Chakrabarti G. 1,4-Benzoquinone (PBQ) induced toxicity in lung epithelial cells is mediated by the disruption of the microtubule network and activation of caspase-3. Chem Res Toxicol. 2010; 23:1054–66. [PubMed: 20499891]
23. Gibaldi, M.; Perrier, D. Phamakokinetics. New York: Marcel Dekker Inc.; 1982.
24. Acharya BR, Bhattacharyya S, Choudhury D, Chakrabarti G. The microtubule depolymerizing agent naphthazarin induces both apoptosis and autophagy in A549 lung cancer cells. Apoptosis. 2011; 16:924–39. [PubMed: 21667044]
25. Mgbonyebi OP, Russo J, Russo IH. Roscovitine induces cell death and morphological changes indicative of apoptosis in MDA-MB-231 breast cancer cells. Cancer Res. 1999; 59:1903–10. [PubMed: 10213499]
26. Chua YS, Chua YL, Hagen T. Structure activity analysis of 2-methoxyestradiol analogues reveals targeting of microtubules as the major mechanism of antiproliferative and proapoptotic activity. Mol Cancer Ther. 2010; 9:224–35. [PubMed: 20053769]
27. Siegel R, Naishadham D, Jemal A. Cancer statistics, 2012. CA Cancer J Clin. 2012; 62:10–29. [PubMed: 22237781]
28. Ricker JL, Chen Z, Yang XP, Pribluda VS, Swartz GM, Van WC. 2-methoxyestradiol inhibits hypoxia-inducible factor 1alpha, tumor growth, and angiogenesis and augments paclitaxel efficacy in head and neck squamous cell carcinoma. Clin Cancer Res. 2004; 10:8665–73. [PubMed: 15623651]
29. Siebert AE, Sanchez AL, Dinda S, Moudgil VK. Effects of estrogen metabolite 2-methoxyestradiol on tumor suppressor protein p53 and proliferation of breast cancer cells. Syst Biol Reprod Med. 2011; 57:279–87. [PubMed: 22077725]

30. Fotopoulou C, Baumunk D, Schmidt SC, Schumacher G. Additive growth inhibition after combined treatment of 2-methoxyestradiol and conventional chemotherapeutic agents in human pancreatic cancer cells. Anticancer Res. 2010; 30:4619–24. [PubMed: 21115915]

31. Dahut WL, Lakhani NJ, Gulley JL, Arlen PM, Kohn EC, Kotz H, et al. Phase I clinical trial of oral 2-methoxyestradiol, an antiangiogenic and apoptotic agent, in patients with solid tumors. Cancer Biol Ther. 2006; 5:22–7. [PubMed: 16357512]

32. James J, Murry DJ, Treston AM, Storniolo AM, Sledge GW, Sidor C, et al. Phase I safety, pharmacokinetic and pharmacodynamic studies of 2-methoxyestradiol alone or in combination with docetaxel in patients with locally recurrent or metastatic breast cancer. Invest New Drugs. 2007; 25:41–8. [PubMed: 16969706]

33. D'Amato RJ, Lin CM, Flynn E, Folkman J, Hamel E. 2-Methoxyestradiol, an endogenous mammalian metabolite, inhibits tubulin polymerization by interacting at the colchicine site. Proc Natl Acad Sci U S A. 1994; 91:3964–8. [PubMed: 8171020]

34. Kamath K, Okouneva T, Larson G, Panda D, Wilson L, Jordan MA. 2-Methoxyestradiol suppresses microtubule dynamics and arrests mitosis without depolymerizing microtubules. Mol Cancer Ther. 2006; 5:2225–33. [PubMed: 16985056]

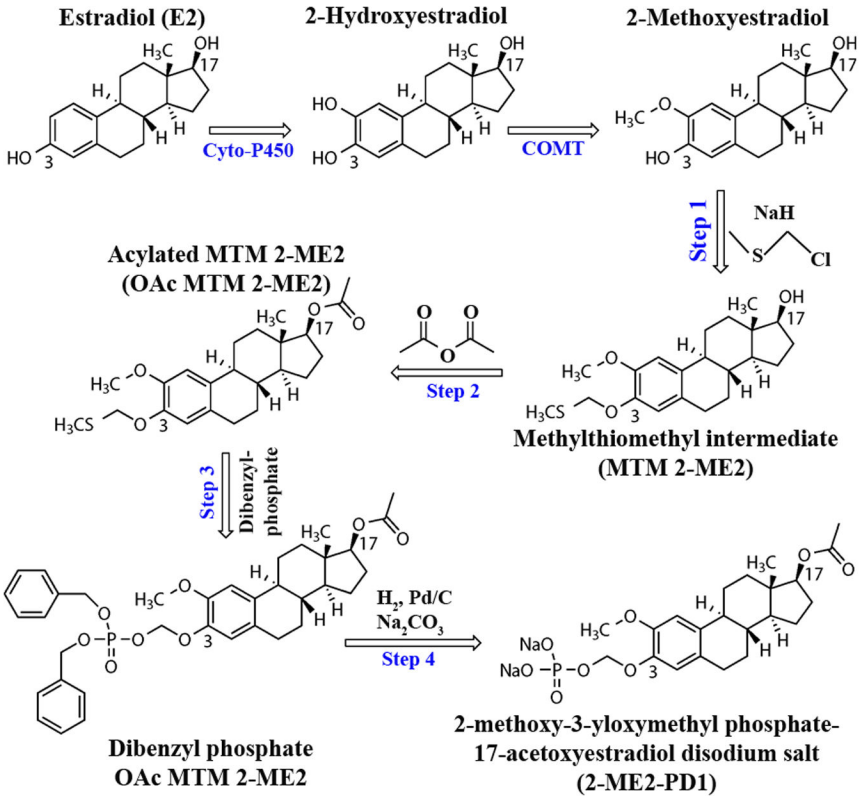

Figure 1. Sequential events of synthesis of the 2-ME2 prodrug, 2-ME2-PD1, from 2-Methoxyestradiol

The first step in the synthesis of 2-ME2-PD1 is the selective formation of the methylthiomethyl ether intermediate at the phenolic hydroxyl of 2-ME2 (selectively favored over the secondary alcohol on the opposite side of the molecule). This step was followed by acylation of the secondary alcohol (to protect and hinder metabolism at C-17 position). The acetylated product was purified by column chromatography and used in the formation of the protected phosphate ester. Final removal of the dibenzyl groups on the phosphate ester (C-3 position) and formation of the sodium salt gives the desired prodrug structure.

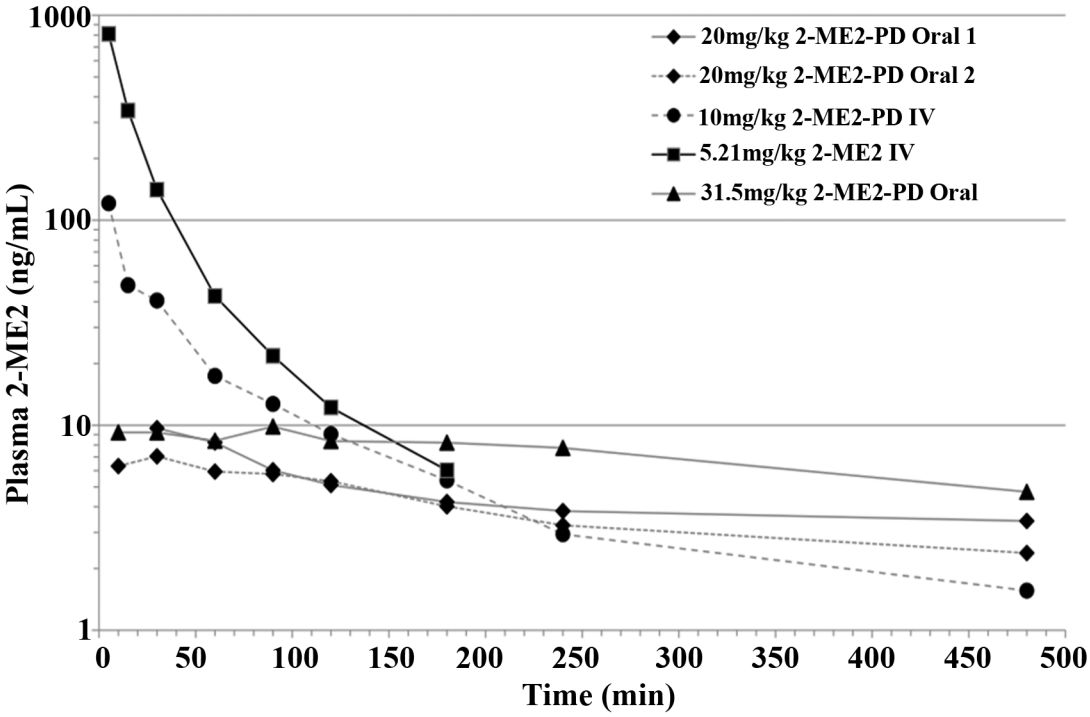

Figure 2. Rat plasma 2-ME2 levels as a function of time following the administration of 2-ME2-PD1 or 2-ME2 by various routes

A cannulated rat model was used to study the plasma 2-ME2 concentrations following oral and intravenous administration of 2-ME2-PD1 relative to 2-ME2.

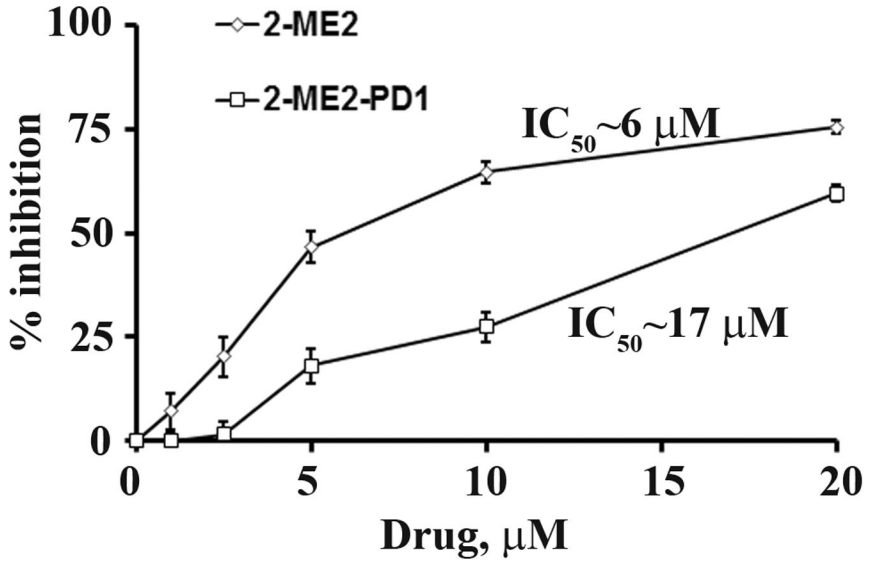

Figure 3. The differential effect of 2-ME2 and 2-ME2-PD1 on OE33 cell proliferation *in vitro*

Approximately 60-70% confluent OE33 cells were grown in the presence or absence of indicated concentrations of 2-ME2 or 2-ME2-PD1 for 48 h, and cellular viability/ proliferation was determined using crystal violet dye colorimetric assay. The values with error bars are expressed as mean ± standard deviation (SD) of three independent experiments *P*- values were determined by Student's *t*-test. **P* <0.001; ***P*<0.0001 versus control.

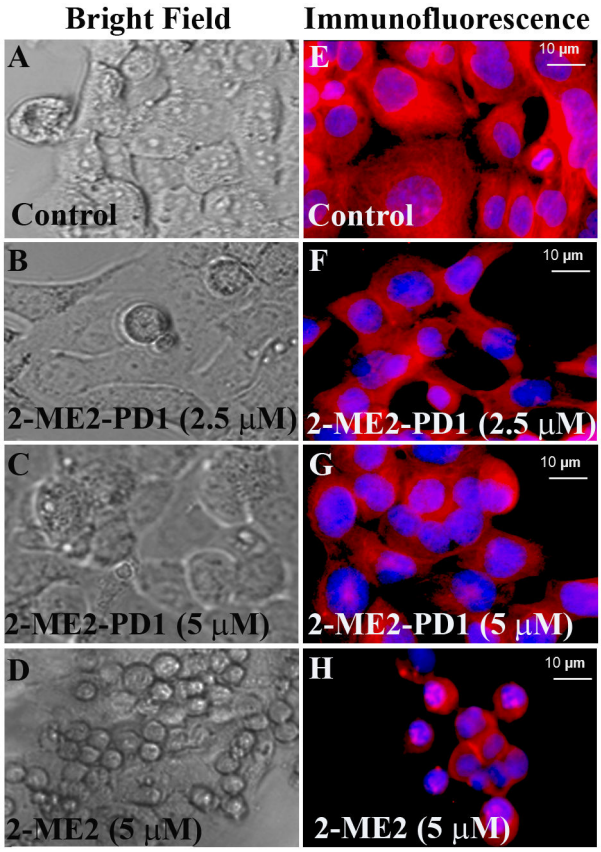

Figure 4. The differential effect of 2-ME2 and 2-ME2-PD1 on cellular morphology and microtubule organization in OE33 cells *in vitro*

To study cellular morphology, semiconfluent OE33 cells were exposed to 2-ME2 or 2-ME2-PD1 for 48 h or left untreated and cellular morphological changes were monitored using a Nikon Eclipse Ti-U phase-contrast microscope **[left panels (A-D)]**. To determine the microtubule disruption by 2-ME2 and 2-ME2-PD1, semiconfluent OE33 cells were exposed to 2-ME2 or 2-ME2-PD1 for 48 h or left untreated. Treated or untreated cells were fixed and stained with TRITC-conjugated antibody to anti-α-Tubulin to visualized microtubules (red) and counterstained with DAPI (4, 6-diamidino-2-phenylindole) to visualize nuclei (blue). Images of the cellular microtubules were captured using a Nikon Eclipse Ti-U fluorescence microscope **[right panels (E-H)]**.

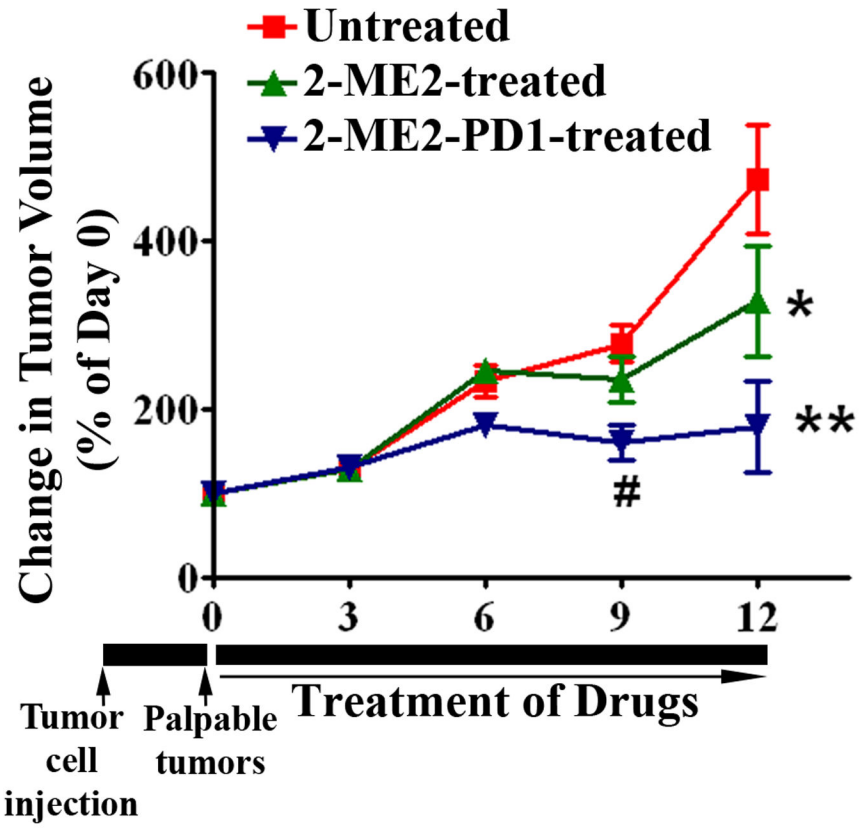

Figure 5. The differential effect of 2-ME2 and 2-ME2-PD1 on OE33 tumor xenografts in nude mice

OE33 cells with Matrigel were injected *sc* into the right hind leg of each athymic nude mice as described in Materials and Methods section. After palpable tumors developed, animals were exposed to 2-ME2 or 2-ME2-PD1 or vehicle alone every day for 12 days. The change in tumor volume is plotted for untreated (control), 2-ME2 treated and 2-ME2-PD1 treated. *Bars*, SD. **P*< 0.01; ***P*<0.001; #*P*<0.005 vs untreated.

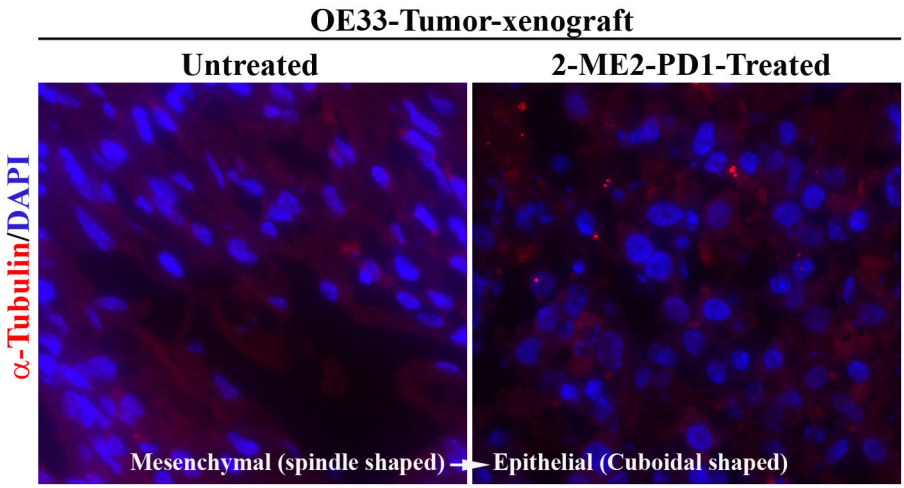

Figure 6. The differential effect of 2-ME2-PD1 on cellular morphology and microtubule organization in OE33-tumor xenograft

2-ME2-PD1-treated or untreated (control) tumor tissue samples were collected and immunofluorescent staining of microtubule filaments (red) in paraffin embedded sections of the tumors was performed using monoclonal anti-α-Tubulin antibody.

Table 1

Summary of 2-ME2 and 2-ME2-PD1 pharmacokinetic parameters

Sprague Dawley rats were implanted with carotid artery, and jugular and/or femoral vein catheters. The Culex Automated Pharmacology System facilitated pharmacokinetic analysis of the resulting plasma concentration-time data was performed using PK Solutions software.

	2-ME2	2-ME2-PD1		
Route	**Intravenous**	**Intravenous**	**Oral**	**Oral**
Dose (mg/kg)	5.21	10	20	31.5
Corrected Dose (mg/kg)	5.21	6.06	12.13	19.11
$AUC_{t\text{-}480}$ ($ng \cdot min \cdot mL^{-1}$)	19253	4967	2006	3516
C_{max} (ng/mL)	1221	121	8.4	9.9
$T_{1/2}$ (min)	59	262	807	411
Bioavailability[1] (%)	100	21.8	4.4	4.9

[1] Bioavailability values are through 480 minutes